Pergamon

Polyhedron Vol. 14, No. 10, pp. 1315–1325, 1995

0277-5387/95 $9.50+0.00

0277-5387(94)00407-2

THREE-DIMENSIONAL HÜCKEL MOLECULAR ORBITAL ENERGY LEVEL CORRELATION DIAGRAMS FOR POLYHEDRAL REARRANGEMENTS

MING ZHAO and BENJAMIN M. GIMARC*

Department of Chemistry and Biochemistry, University of South Carolina, Columbia, SC 29208, U.S.A.

(*Received* 2 *June* 1994; *accepted* 5 *October* 1994)

Abstract—A three-dimensional Hückel method recently developed for cluster compounds has been used to investigate polyhedral rearrangements of organic molecules as well as main-group inorganic clusters. The method starts from information about atomic connectivity and number of cluster electrons, familiar and convenient concepts for chemists. Calculations lead to diagrams that show how molecular orbital (MO) energy levels and second moment scaled total energies correlate between different structural forms. We consider diamond–square–diamond (DSD) framework reorganization mechanisms for pseudo-rotations of the closo-boranes. For $B_5H_5^{2-}$ and $B_9H_9^{2-}$, the single DSD mechanism is not allowed by the principle of conservation of orbital symmetry. DSD rearrangements are allowed for the other closo-boranes we studied here, with increasing activation energies, $B_8H_8^{2-} \sim B_{11}H_{11}^{2-} < B_7H_7^{2-} \sim B_{10}H_{10}^{2-} < B_6H_6^{2-}$, depending on the number of square faces opened during rearrangement. MO correlation diagrams and corresponding total energy curves for various numbers of cluster electrons provide visual rationalizations of observed structural trends with different numbers of cluster electrons. In particular, we discuss framework reorganizations for square to tetrahedron, hexagon to trigonal prism, hexagon to octahedron and cube to square antiprism.

We have recently developed a three-dimensional Hückel method for cluster compounds and used it to calculate some of the properties of the closo-boranes and -carboranes.[1–3] The successes of these applications have encouraged us to use the method more widely. In this paper, we present molecular orbital (MO) energy level correlation diagrams calculated by the three-dimensional Hückel method for several examples of polyhedral rearrangements. Because the closo-boranes and -carboranes exhibit many different possibilities for such rearrangements, which have been studied by experimental and more complete theoretical methods, most of the examples we have chosen here involve the boranes and carboranes, but we have also included examples of polyhedral rearrangements from organic chemistry and main-group inorganic chemistry.

THREE-DIMENSIONAL HÜCKEL THEORY

The three-dimensional Hückel theory is a true successor to the two-dimensional Hückel theory that has been useful as a basis for qualitative interpretations of structures and properties in planar conjugated hydrocarbons, as well as related planar inorganic molecules and ions.[4–8] The information required to initiate a calculation consists of little more than the number of electrons involved in cluster bonding and an adjacency matrix that specifies bonds between atoms.

The atomic orbital (AO) basis set for three-dimensional Hückel theory for clusters has been described by Wade[9] and King and Rouvray.[10] Of the four valence AOs contributed by each of the *n*

*Author to whom correspondence should be addressed.

skeletal atoms, one is involved in a normal electron pair bond to a ligand or holds an unshared electron pair, and is therefore not available for cluster bonding. Of the remaining three valence AOs, one is an internal radial hybrid that points toward the centre of the cluster, while the other two are p AOs that are tangential to the sphere that can be imagined as enclosing the polyhedron. These $3n$ AOs X_r can be combined to make a set of $3n$ MOs ϕ_i for cluster bonding. Choices of coulomb, resonance and overlap integrals follow standard Hückel assumptions. For homoatomic clusters, coulomb integrals for all atoms are the same:

$$H_{rr} = \langle X_r|H|X_r\rangle = \alpha.$$

Resonance integrals are related to a standard value such that

$$H_{rs} = \langle X_r|H|X_s\rangle = \beta$$

if atoms r and s are bonded to each other and $H_{rs} = 0$ otherwise. The AOs are assumed to be normalized but overlap integrals involving AOs on different atoms are completely neglected:

$$S_{rs} = \langle X_r|X_s\rangle = \begin{cases} 1, & r = s \\ 0, & r \neq s \end{cases}.$$

Solution of the resulting secular determinant

$$|H_{rs} - \varepsilon_i S_{rs}| = 0$$

gives the MOs ϕ_i and their energies ε_i. Burdett and Lee have shown that second moment scaling of the sum of individual electron orbital energies gives improved results for the comparisons of total energies, particularly of structures containing different numbers of bonds.[11-14] Therefore, we take

$$E = \gamma \sum_i \varepsilon_i,$$

where E is the total energy with the sum over all electrons and γ is the second moment scaling factor,

$$\gamma = \left[\sum_i \varepsilon_i^2 \text{ (reference structure)} / \sum_i \varepsilon_i^2\right]^{1/2}.$$

As the reference structure, we have chosen the corresponding n-vertex deltahedron.

POLYHEDRAL REARRANGEMENTS

Equation (1) shows the degenerate rearrangement or pseudo-rotation of a trigonal bipyramid through a square pyramid structure by a diamond–square–diamond (DSD) process.[15-17]

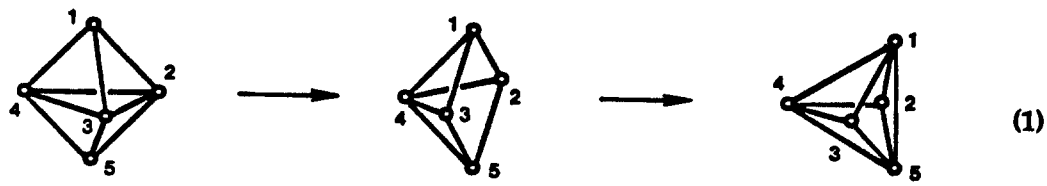

(1)

We can model this rearrangement with the three-dimensional Hückel method by varying the resonance integrals β_{23} and β_{15} of the bonds that are broken and formed during the process. Consider a parameter that varies between $t = 0$ (no bond between atoms 1 and 5) and $t = 1$ (fully formed 1–5 bond). Let $\beta_{15} = t\beta$ and $\beta_{23} = (1-t)\beta$. Figure 1 shows how three-dimensional Hückel MO energy

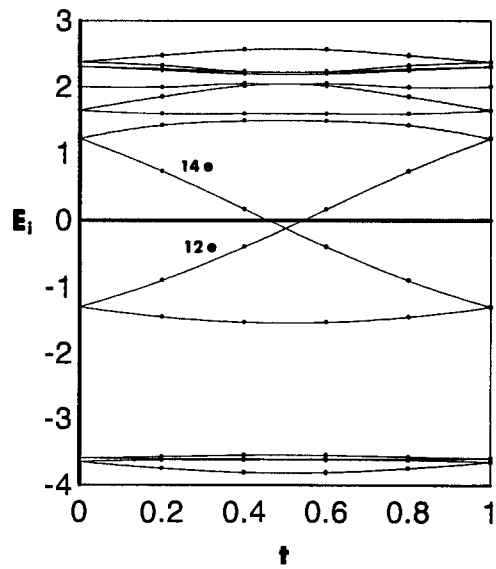

Fig. 1. MO energy level correlations from three-dimensional Hückel theory following eq. (1); the degenerate rearrangement of a trigonal bipyramid ($t = 0$ and 1) through a square pyramidal intermediate ($t = 0.5$). For $B_5H_5^{2-}$ (12 cluster electrons), HOMO–LUMO crossing makes the rearrangement symmetry forbidden.

levels for the five-atom cluster change as functions of the parameter t through the rearrangement of eq. (1). For $B_5H_5^{2-}$ (12 cluster bonding electrons) electron configurations of reactant ($t = 0$) and product ($t = 1$) are identical, but the HOMO and LUMO cross at the square pyramid transition state structure ($t = 0.5$), indicating that the DSD framework reorganization for $B_5H_5^{2-}$ is symmetry forbidden.[18] Although $B_5H_5^{2-}$ has never been prepared, two of the three possible isomers of the isoelectronic carborane $C_2B_3H_5$ are known to have trigonal bipyramidal shapes.[19,20] Interconversion of these isomers does not occur; on heating, they decompose.[21] The homoatomic clusters Tl_5^{7-}, Sn_5^{2-}, Pb_5^{2-} and Bi_5^{3+} (12 cluster bonding electrons) also prefer trigonal bipyramidal geometry.[22-24] The Bi_5^+ cation has been observed in mass spectra.[25] From the slopes of MO curves in Fig. 1, it is apparent that Bi_5^+, with 14 cluster electrons, can be expected to have square pyramidal geometry. These structure conclusions are reinforced by the second moment scaled total energies E, shown in Fig. 2 as functions of the parameter t. The minimum total energy for the 12-electron cluster is in the form of a trigonal bipyramid, $t = 0$ and 1, while the 14-electron cluster has minimum energy in the square pyramid shape, $t = 0.5$.

Equation (2) is the degenerate rearrangement of the octahedron through a trigonal prism by a triple DSD process:

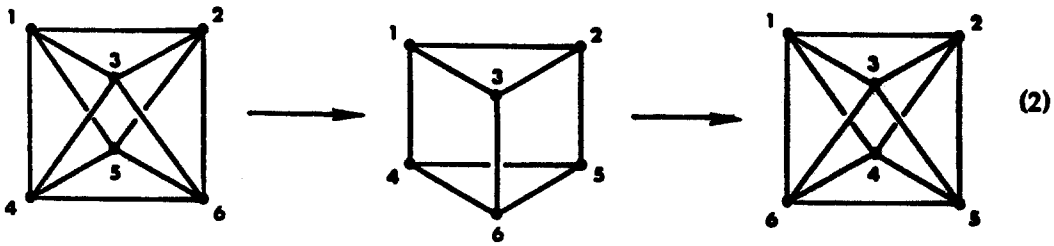

Let $\beta_{16} = \beta_{24} = \beta_{35} = t\beta$ and $\beta_{15} = \beta_{26} = \beta_{34} = (1-t)\beta$. Figure 3 displays the changes in three-dimensional Hückel MO energies as t varies from 0 to 1. For $B_6H_6^{2-}$ (14 cluster electrons) no HOMO–LUMO crossings occur and the rearrangement is symmetry allowed, but a sizeable activation barrier presents itself as the trigonal prism intermediate ($t = 0.5$). $B_6H_6^{2-}$ is not fluxional. The two possible isomers of the isoelectronic and isostructural carborane $C_2B_4H_6$ have been prepared and the higher energy 1,6-isomer has been observed to rearrange to the lower energy isomer on heating at 250°C.[26]

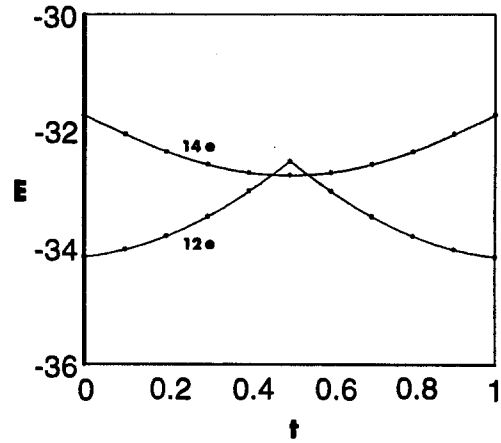

Fig. 2. Total energies E with second moment scaling as a function of t for five-atom clusters containing 12 and 14 electrons. The cusp at $t = 0.5$ (square pyramid) for the 12-electron cluster is a result of the HOMO–LUMO crossing shown in Fig. 1. The 14-electron cluster has minimum energy as a square pyramid.

$C_2B_4H_6$ probably does not rearrange by eq. (2). McKee, using *ab initio* SCF MO calculations, has recently described a more likely mechanism that passes through other transition state and intermediate structures and has a calculated activation energy that agrees with the experimental value.[27]

Although the naked cluster Sn_6^{2-} is unknown, it would be isoelectronic with $B_6H_6^{2-}$. The related six-atom tin cluster $Sn_6R_6^{2-}$, R = $Cr(CO)_5$, has been prepared and found to have the expected octahedral geometry.[28] No six-atom clusters with 16 cluster electrons are known. The low-dipping MO in Fig. 3 that is filled at the 18-electron level is doubly degenerate, so a 16-electron cluster in the system of eq. (2) would have an open-shell electron configuration and would be unlikely. For As_6 (18 cluster electrons), the trigonal prism has the lowest energy of several plausible structures tested by *ab initio* SCF MO calculations.[29] The cation Te_6^{4+} (20 cluster electrons) has been prepared; X-ray diffrac-

tion studies show that Te_6^{4+} has a trigonal prism shape.[30] Total energies in Fig. 4 are lowest for the 14-electron cluster as an octahedron ($t = 0$ and 1); 18- and 20-electron clusters have minimum energies as triangular prisms ($t = 0.5$).

Equation (3) is the concerted double DSD process for the degenerate rearrangement of the pentagonal pyramid through a capped triangular prism:

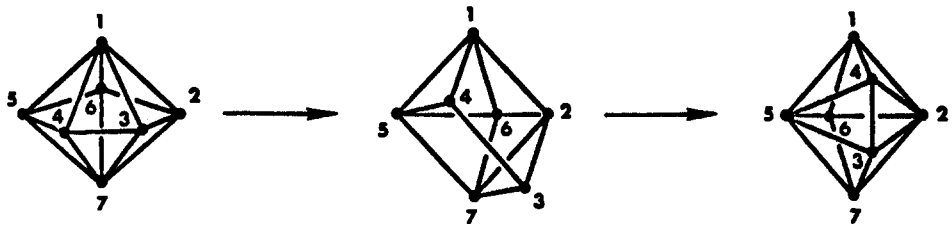

(3)

Assume $\beta_{24} = \beta_{35} = t\beta$ and $\beta_{13} = \beta_{47} = (1-t)\beta$. Figure 5 is the correlation diagram for MO energies along eq. (3) as the parameter t varies from 0 to 1. Figure 6 is the corresponding total energy for a 16-electron cluster. $B_7H_7^{2-}$ (16 electrons) is a pentagonal bipyramid. Figure 5 shows that the rearrangement of $B_7H_7^{2-}$ is symmetry allowed. The HOMO presents an activation barrier (shown in Fig. 6) to the process, but this barrier is smaller than that in Fig. 4, a result that is consistent with the fact that eq. (3) opens only two square faces to give the capped triangular prism transition state, while eq. (2) opens three square faces to produce a trigonal prism. Although $B_7H_7^{2-}$ is not fluxional, isomerization of derivatives of the corresponding carborane, 2,3-$C_2B_5H_7$ to 2,4-$C_2B_5H_7$, has been observed.[31,32] Other considerations suggest that a variation of eq. (3), in which square faces open and close sequentially rather than simultaneously, should have a lower activation barrier.[3]

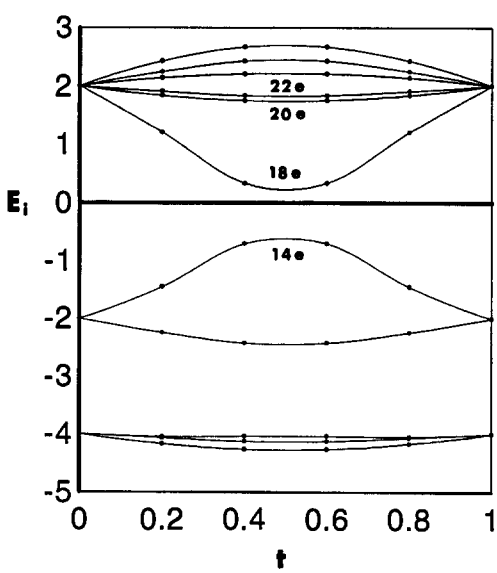

Fig. 3. MO energy level correlations for the degenerate rearrangement of an octahedron ($t = 0$ and 1) by way of a trigonal prism intermediate ($t = 0.5$), eq. (2). For $B_6H_6^{2-}$ (14 electrons), this process is symmetry allowed, but the HOMO presents a large activation barrier.

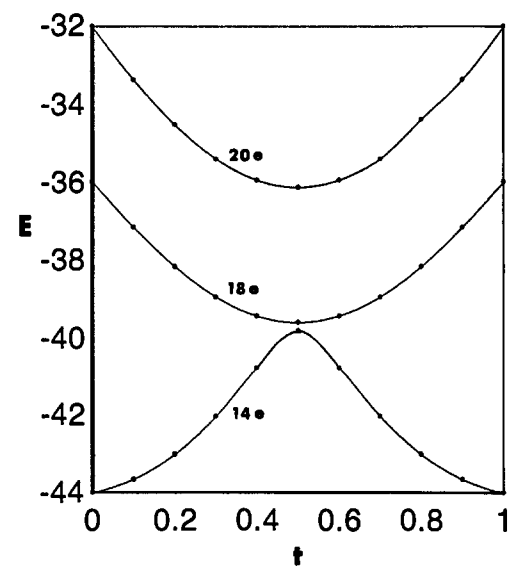

Fig. 4. Total energy E for the six-atom cluster is lowest for 14 electrons in the octahedral shape ($t = 0$ and 1). The minimum for 18 and 20 cluster electrons occurs at trigonal prism geometry ($t = 0.5$).

Equation (4) illustrates the degenerate rearrangement of the eight-atom disbisphenoid cluster through a bicapped triangular prism intermediate by a single DSD process:

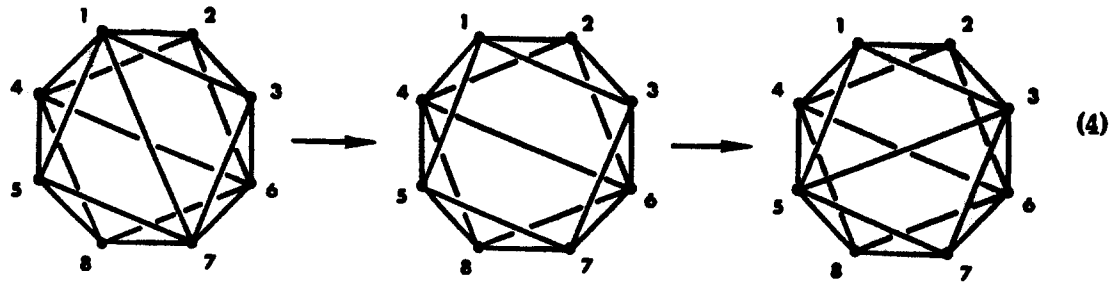

Let $\beta_{35} = t\beta$ and $\beta_{17} = (1-t)\beta$. Figure 7 shows the correlation of MO energies as t varies from 0 to 1. It is easy to see from Fig. 7 that the rearrangement of $B_8H_8^{2-}$ (18 electrons) is symmetry allowed and should have a very low activation energy, which is supported by the broad, low hump of the total energy curve in Fig. 8. Indeed, $B_8H_8^{2-}$ is known to be fluxional with a very low activation barrier to rearrangements.[33]

Equation (5) portrays the degenerate rearrange-

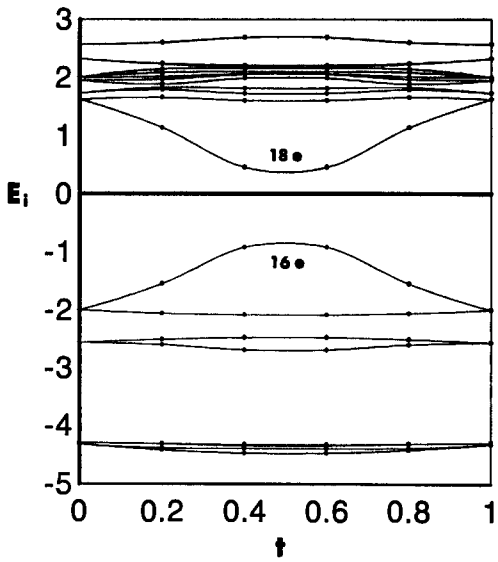

Fig. 5. MO energy level correlations for the double DSD process of eq. (3). At the 16-electron level ($B_7H_7^{2-}$) the process is allowed, but the activation energy is relatively high.

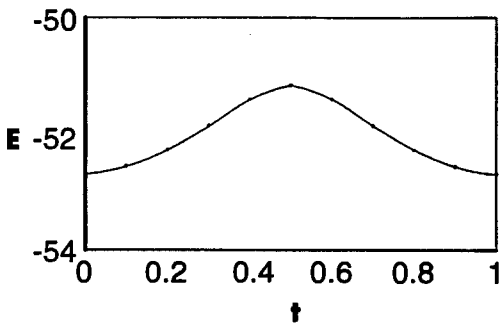

Fig. 6. The minimum total energy of the seven-atom cluster containing 16 electrons occurs for the pentagonal bipyramid ($t = 0$ and 1) with a maximum for the activation barrier to degenerate rearrangement at the capped triangular prism ($t = 0.5$).

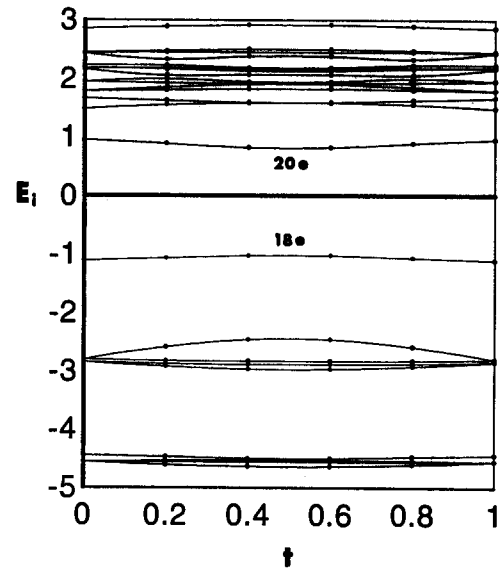

Fig. 7. MO energy level correlations following the degenerate rearrangement described by eq. (4). For $B_8H_8^{2-}$ (18 electrons), the process is allowed with low activation energy.

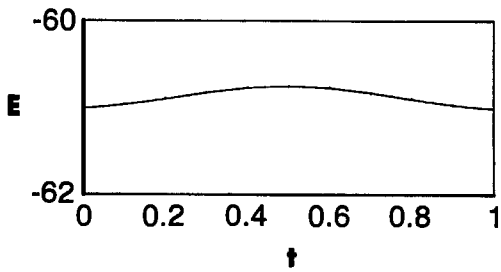

Fig. 8. Total energy of the eight-atom disbisphenoid cluster with 18 electrons shows a very low activation barrier to degenerate rearrangement through a DSD process.

ment of a tricapped trigonal prism by a single DSD process passing through a unicapped square antiprism:

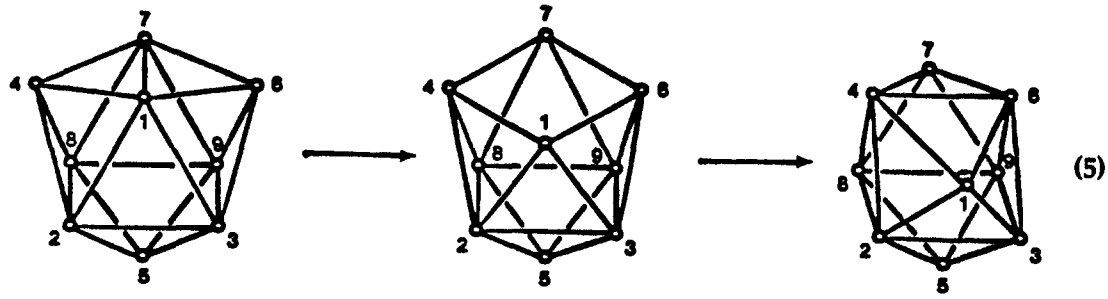

Figure 9 shows the MO correlation diagram that results from setting $\beta_{46} = t\beta$ and $\beta_{17} = (1-t)\beta$ and varying t from 0 to 1. Figure 10 shows total energies of 20- and 22-electron clusters over the same interval of t. $B_9H_9^{2-}$ (20 cluster electrons) has the structure of the tricapped trigonal prism.[34] The degenerate rearrangement of $B_9H_9^{2-}$ by eq. (5) is symmetry forbidden as implied by the HOMO–LUMO crossing at $t = 0.5$. $B_9H_9^{2-}$ is not fluxional. A double DSD process is symmetry allowed,[35] but it would have an activation barrier to rearrangement comparable with that for $B_7H_7^{2-}$. Only one isomer of the isoelectronic and isostructural carborane, $C_2B_7H_9$, has been reported.

The cluster Ge_9^{2-} is isostructural and isoelectronic with $B_9H_9^{2-}$.[36] X-ray diffraction analyses show that the ions Ge_9^{4-} and Sn_9^{4-} (22 electrons) have unicapped square antiprism structures in the crystal, corresponding to filled degenerate HOMOs at $t = 0.5$.[36,37] But Sn_9^{4-} is fluxional in solution.[38] One X-ray structural determination describes the Sn_9^{4-} polyhedron as having geometry between the tricapped trigonal prism and the unicapped square antiprism.[39] The 22-electron Bi_9^{5+} cluster has the tricapped trigonal prism structure of Ge_9^{2-} with two electrons fewer.[40] Figure 9 shows that interconversion of these two structures at the 22-electron level is symmetry allowed and of low activation energy. The total energy of the 22-electron cluster has a shallow minimum at $t = 0.5$ (capped square antiprism) in Fig. 10, while the cusp or spike of the 20-electron curve at $t = 0.5$ indicates the intersection of HOMO and LUMO.

We have carried out three-dimensional Hückel calculations for degenerate rearrangements of $B_{10}H_{10}^{2-}$ and $B_{11}H_{11}^{2-}$. Results are in agreement with previous findings based on extended Hückel and *ab initio* calculations.[41,42] Degenerate rearrangements for $B_{10}H_{10}^{2-}$ and $B_{11}H_{11}^{2-}$ are allowed. The correlation and total energy diagrams for the single

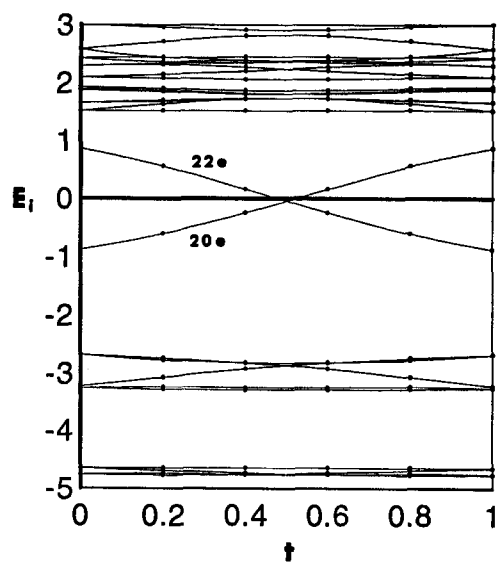

Fig. 9. MO energy correlations for the pseudo-rotation specified by eq. (5) for a nine-atom cluster. HOMO–LUMO crossings at the 20-electron level prohibit this rearrangement for $B_9H_9^{2-}$, but for clusters with 22 electrons the process is allowed and observed.

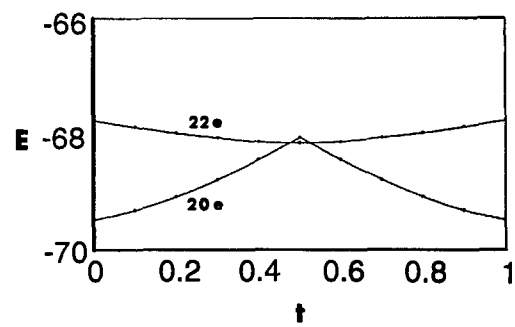

Fig. 10. Total energies for the nine-atom cluster show a symmetry forbidden DSD rearrangement for the 20-electron cluster tricapped trigonal prism and a broad flat energy minimum for the 22-electron cluster as a capped square antiprism ($t = 0.5$).

DSD pseudo-rotation of $B_{11}H_{11}^{2-}$ look much like Figs 7 and 8 for $B_8H_8^{2-}$ or Figs 9 and 10 (22-electron level, Sn_9^{4-}). $B_{11}H_{11}^{2-}$ is known to be fluxional with a very low activation energy for rearrangement. The degenerate rearrangement of $B_{10}H_{10}^{2-}$ requires a double DSD process and the corresponding correlation and total energy diagrams resemble Figs 5 and 6 for $B_7H_7^{2-}$. Rearrangements of known $C_2B_8H_{10}$ isomers have been observed.

Equation (6) shows the conversion of a square planar structure to a regular tetrahedron through a puckered square:

(6)

Let $\beta_{13} = \beta_{24} = t\beta$, where $t = 0$ is the square and $t = 1$ is the tetrahedron. Figure 11 is the MO correlation diagram for the square to tetrahedron conversion and Fig. 12 contains the corresponding total energy curves for eight-, 12-, 14- and 16-electron clusters. With eight cluster electrons, B_4H_4 should be tetrahedral rather than square planar according to Figs 11 and 12. Although B_4H_4 has never been prepared, the results of more advanced quantum mechanical calculations indicate that it should be tetrahedral.[43] Similar considerations suggest that P_4 (12 electrons) should be tetrahedral, the structure long known for this molecule as well as isoelectronic Tl_4^{8-}, Si_4^{4-}, and many others.[44-46] In Fig. 12, dashed curves indicate total energies of clusters with half-filled HOMOs (open-shell electron configurations), while solid curves denote filled HOMOs (closed shells). The closed shell portion of the total energy curves for the 12-electron cluster goes to lowest energy at $t = 1$ (tetrahedron). S_4^{2+}, with 14 electrons, should be square planar rather than tetrahedral. The X-ray diffraction structure of S_4^{2+} shows that it is indeed square, as are Se_4^{2+} and Te_4^{2+}.[47-49] *Ab initio* calculations show that cyclic S_4 (16 electrons) is a puckered square.[50] Cyclobutane, C_4H_8, isoelectronic with S_4, is well known to be a puckered square. At the 16-electron level, the sums of energies of individual electrons are the same (-32β) for both square ($t = 0$) and tetrahedron ($t = 1$), but the second moment scaling factor is greater at $t = 0$ ($\gamma = 1.2247$) than for $t = 1$ ($\gamma = 1.0$) and, as a result, the total energy curve for 16 electrons in Fig. 12 sweeps to a shallow minimum at $t = 0$.

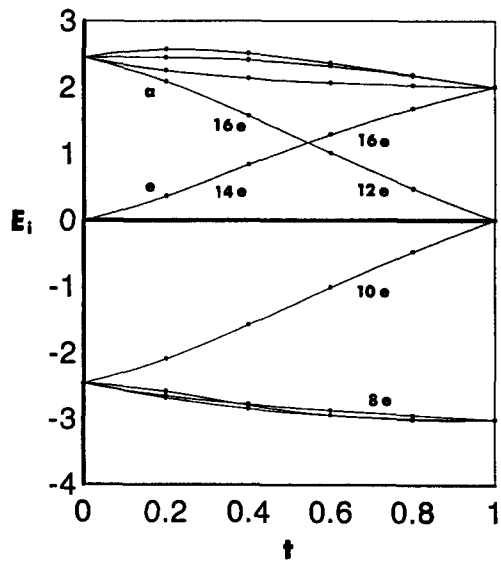

Fig. 11. MO energy level correlations for the conversion of a square ($t = 0$) to a tetrahedron ($t = 1$) by eq. (6).

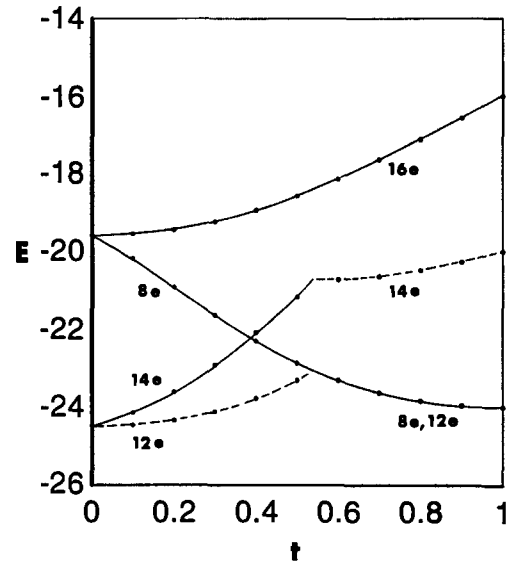

Fig. 12. Total energies of four-atom clusters for shapes linking the square ($t = 0$) and the tetrahedron ($t = 1$). Dashed curves indicate total energies of clusters with half-filled HOMOs (open-shell electron configurations), while solid curves denote filled HOMOs (closed shells).

Equation (7) represents the conversion of a planar hexagon through a non-planar boat form to the trigonal prism:

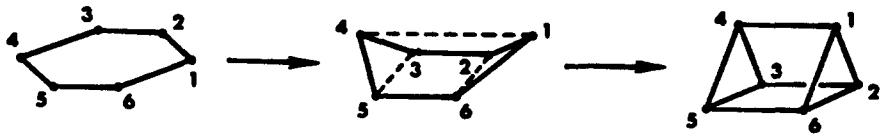

(7)

Set $\beta_{14} = \beta_{26} = \beta_{35} = t\beta$ and let t vary from 0 (planar hexagon) to 1 (trigonal prism). Figure 13 shows how MO energy levels correlate as functions of the parameter t. Figure 14 traces the total energy of the 18-electron cluster. C_6H_6 and As_6 are both 18-electron clusters. For C_6H_6, both planar hexagonal and trigonal prism forms have been prepared, with the hexagonal shape much preferred. *Ab initio* calculations for As_6 show that the trigonal prism is lower in energy than the planar hexagon.[29] Differences in these results have been attributed to differences in strain energies.[29,51] Interconversion of prism and hexagon at the 18-electron level is blocked by HOMO–LUMO crossing near $t = 0.5$ in Fig. 13. This crossing results in a cusp in the total energy in Fig. 14. Second-moment scaling gives additional weight to the total energy of the hexagon ($\gamma = 1.4142$, $t = 0$) compared with that of the trigonal prism ($\gamma = 1.1547$, $t = 1$).

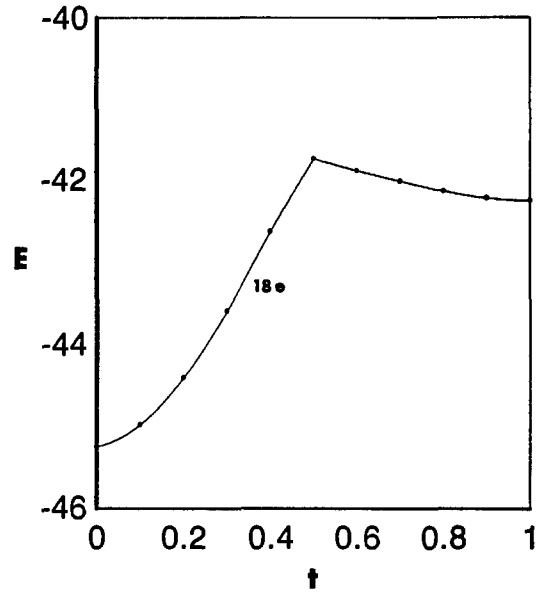

Fig. 14. Total energies of the six-atom, 18-electron cluster in shapes linking the planar hexagon ($t = 0$) and the trigonal prism ($t = 1$).

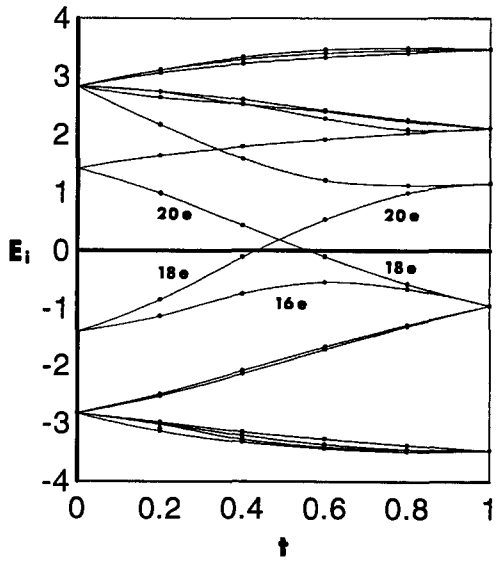

Fig. 13. MO energy level correlations for rearrangement, eq. (7), of a hexagon ($t = 0$) to a triangular prism ($t = 1$) through the boat conformation.

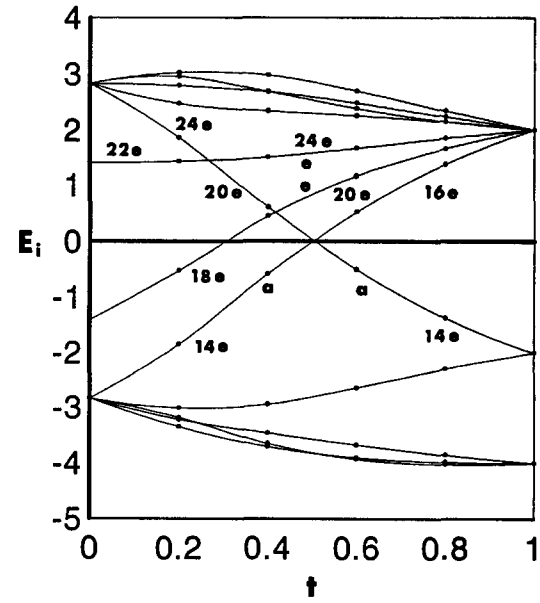

Fig. 15. MO energy level correlations for rearrangement, eq. (8), of a hexagon ($t = 0$) to an octahedron ($t = 1$) through the chair conformation.

Equation (8) describes the folding of a planar hexagon through a chair form to regular octahedron:

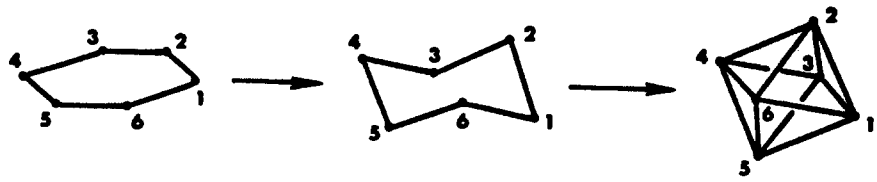

(8)

Let $\beta_{15} = \beta_{13} = \beta_{24} = \beta_{46} = \beta_{26} = \beta_{35} = t\beta$ and vary t from 0 to 1. Figures 15 and 16 are the resulting MO energy correlation diagram and energy curves, respectively. $B_6H_6^{2-}$, with 14 cluster electrons, has the lowest energy in the octahedral shape. At the 14-electron level the chair-form non-planar hexagon is higher in energy, but is protected from rearrangement to the octahedron by HOMO–LUMO crossings at $t = 0.5$. The chair form of $B_6H_6^{2-}$ is unknown. Benzene, 18 electrons, is stable as a planar hexagon. The 18-electron octahedron would have an open-shell electron configuration. At 24 cluster electrons, S_6 and Se_6 as well as isoelectronic cyclohexane, C_6H_{12}, have chair-form structures.[52,53] These should occur at the crossing of a and e MOs near $t = 0.3$ at the 24-electron level in Fig. 15 and the minimum in total energy in Fig. 16.

Equation (9) shows the conversion of a cube to a square antiprism:

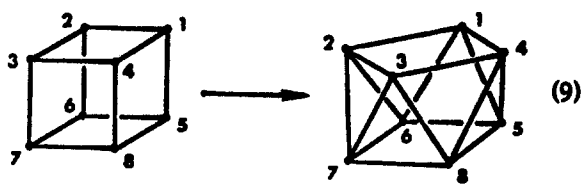

(9)

Let $\beta_{16} = \beta_{27} = \beta_{38} = \beta_{45} = t\beta$ and vary the parameter from $t = 0$ (cube) to $t = 1$ (square antiprism). Figures 17 and 18 are the corresponding MO correlation diagram and total energy curves, respectively. Bi_8^{2+} (22 electrons) has the shape of a square antiprism.[54] The total energy of the 22-electron cluster in Fig. 18 shows a very shallow minimum near $t = 0.5$, very slightly lower than for square antiprism geometry at $t = 1$. Cubane, C_8H_8 (24 electrons), would have an open-shell configuration as a square antiprism but a closed-shell configuration as a cube.[55] At the 24-electron level, rearrangement of the cube to the square antiprism is blocked by HOMO–LUMO crossings near $t = 0.7$.

CONCLUSIONS

These examples of MO correlation diagrams and total energy curves for polyhedral rearrangements illustrate the versatility and utility of the three-dimensional Hückel method. The method starts from information about atomic connectivity and number of cluster electrons, familiar and convenient concepts for chemists. Using a single parameter to modify connectivity among atoms and to describe structural rearrangements can produce

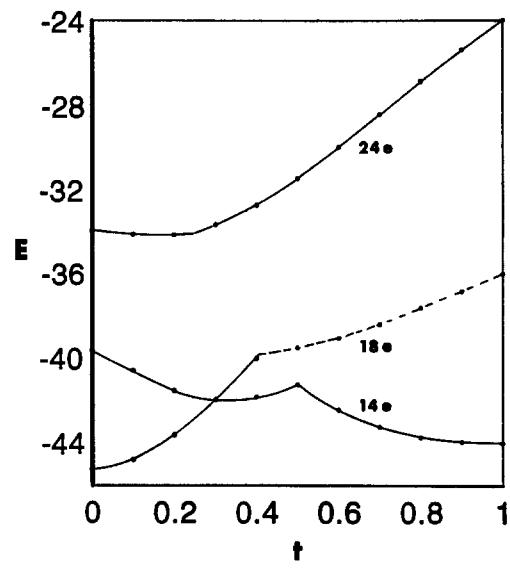

Fig. 16. Total energies of the six-atom cluster in shapes connecting the planar hexagon ($t = 0$) and the octahedron ($t = 1$).

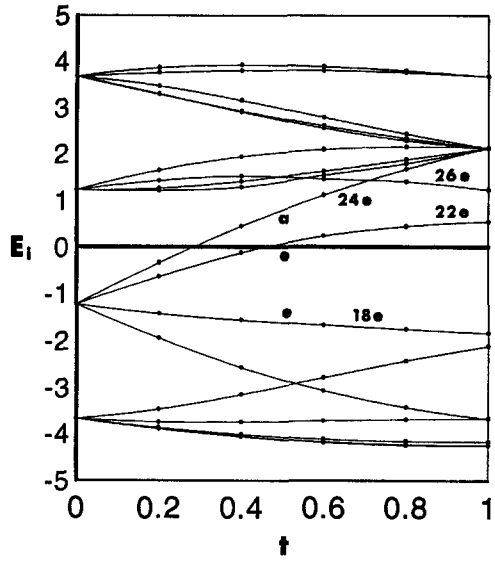

Fig. 17. MO energy level correlations for the polyhedral rearrangement of a cube ($t = 0$) to a square antiprism ($t = 1$), eq. (9).

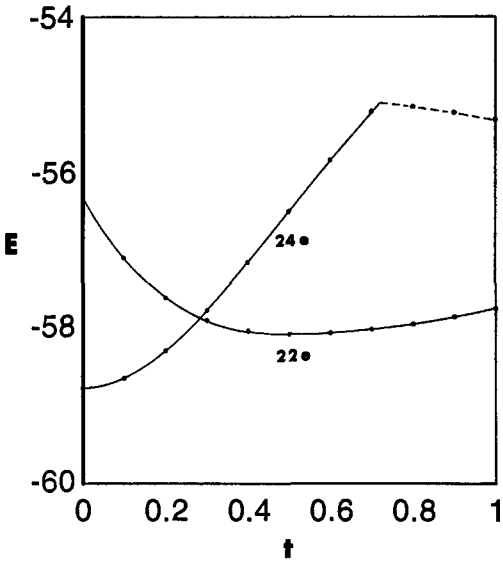

Fig. 18. Total energies of the eight-atom cluster in shapes relating the cube ($t = 0$) and the square antiprism ($t = 1$).

MO energy correlation diagrams and total energies that model extended Hückel diagrams and the structures of real systems. From our correlation diagrams, we can get a qualitative appreciation of activation barriers to polyhedral rearrangements and visualize and rationalize structural trends with numbers of cluster electrons.

Acknowledgements—We are grateful to the National Science Foundation for partial support of this research through Grant No. CHE-9012216 to the University of South Carolina.

REFERENCES

1. M. Zhao and B. M. Gimarc, *Inorg. Chem.* 1993, **32**, 4700.
2. J. Joseph, B. M. Gimarc and M. Zhao, *Polyhedron* 1993, **12**, 2841.
3. B. M. Gimarc and M. Zhao, *Inorg. Chem.*, submitted.
4. A. Streitwieser Jr., *Molecular Orbital Theory for Organic Chemists*. Wiley, New York (1961).
5. C. A. Coulson, B. O'Leary and R. B. Mallion, *Hückel Theory for Organic Chemists*. Academic Press, New York (1978).
6. C. A. Coulson and T. W. Dingle, *Acta Cryst.* 1968, **B24**, 153.
7. B. M. Gimarc and N. Trinajstic, *Pure Appl. Chem.* 1980, **52**, 1443.
8. B. M. Gimarc, *Croat. Chem. Acta* 1984, **57**, 955.
9. K. Wade, *J. Chem. Soc., Chem. Commun.* 1971, 792; *Adv. Inorg. Chem. Radiochem.* 1976, **18**, 1.
10. R. B. King and D. H. Rouvray, *J. Am. Chem. Soc.* 1977, **99**, 7834.
11. J. K. Burdett and S. Lee, *J. Am. Chem. Soc.* 1985, **107**, 3050, 3063.
12. S. Lee, *Inorg. Chem.* 1992, **31**, 3063.
13. S. Lee, *Accts Chem. Res.* 1991, **24**, 249.
14. S. Lee, L. M. Hoistad and S. T. Carter, *New J. Chem.* 1992, **16**, 651.
15. W. N. Lipscomb, *Science* 1966, **153**, 373.
16. R. B. King, *Inorg. Chim. Acta* 1981, **49**, 237; *Theor. Chim. Acta* 1984, **64**, 439.
17. E. L. Muetterties, *Tetrahedron* 1974, **30**, 1595.
18. B. M. Gimarc and J. J. Ott, *Inorg. Chem.* 1986, **25**, 83.
19. I. Shapiro, C. D. Good and R. E. Williams, *J. Am. Chem. Soc.* 1962, **84**, 3837.
20. R. N. Grimes, *J. Am. Chem. Soc.* 1966, **88**, 1070.
21. R. N. Grimes, *J. Organomet. Chem.* 1967, **8**, 45.
22. Z. Dong and J. D. Corbett, *J. Am. Chem. Soc.* 1994, **116**, 3429.
23. P. A. Edwards and J. D. Corbett, *Inorg. Chem.* 1977, **16**, 903.
24. J. D. Corbett, *Inorg. Chem.* 1968, **7**, 198.
25. M. E. Gensic, R. R. Freeman and M. A. Duncan, *J. Chem. Phys.* 1988, **89**, 223.
26. T. Onak, R. P. Drake and G. B. Dunks, *Inorg. Chem.* 1964, **3**, 1686.
27. M. L. McKee, *J. Am. Chem. Soc.* 1992, **114**, 879.
28. B. Schiemenz and G. Huttner, *Angew. Chem., Int. Edn Engl.* 1993, **32**, 297.
29. D. S. Warren, B. M. Gimarc and M. Zhao, *Inorg. Chem.* 1994, **33**, 710.
30. R. J. Gillespie, W. Luk and D. R. Slim, *J. Chem. Soc., Chem. Commun.* 1976, 791; R. C. Burns, R. J. Gillespie, W.-C. Luk and D. R. Slim, *Inorg. Chem.* 1979, **18**, 3086.

31. J. S. Beck, and A. P. Zahn and L. G. Sneddon, *Organometallics* 1986, **5**, 2552.
32. Z. J. Abdou, G. Abdou, T. Onak and S. Lee, *Inorg. Chem.* 1986, **25**, 2678.
33. E. L. Muetterties, R. J. Wiersema and M. F. Hawthorne, *J. Am. Chem. Soc.* 1973, **95**, 7520.
34. L. J. Guggenberger, *Inorg. Chem.* 1968, **7**, 2260.
35. B. M. Gimarc and J. J. Ott, *Inorg. Chem.* 1986, **25**, 2708.
36. C. H. E. Belin, J. D. Corbett and A. Cisar, *J. Am. Chem. Soc.* 1977, **99**, 7163.
37. J. D. Corbett and P. A. Edwards, *J. Chem. Soc., Chem. Commun.* 1975, 984; *J. Am. Chem. Soc.* 1977, **99**, 3313.
38. R. W. Rudolph, W. L. Wilson, F. Parker, R. C. Taylor and D. C. Young, *J. Am. Chem. Soc.* 1978, **100**, 4629.
39. L. Diehl, K. Khodadadeh, D. Kummer and J. Strähle, *Chem. Ber.* 1976, **109**, 33404; *Z. Naturfor.* 1976, **B31**, 522.
40. A. Hershaft and J. D. Corbett, *Inorg. Chem.* 1963, **2**, 979; R. M. Friedman and J. D. Corbett, *Inorg. Chem.* 1973, **12**, 1134.
41. B. M. Gimarc and J. J. Ott, *J. Am. Chem. Soc.* 1987, **109**, 1388.
42. B. M. Gimarc, B. Dai, D. S. Warren and J. J. Ott, *J. Am. Chem. Soc.* 1990, **112**, 2597.
43. W. M. Lipscomb, *Pure Appl. Chem.* 1980, **52**, 1.
44. L. R. Maxwell, S. B. Hendricks and V. M. Mosley, *J. Chem. Phys.* 1935, **3**, 699.
45. D. A. Hansen and J. F. Smith, *Acta Cryst.* 1967, **22**, 836.
46. E. Busmann, *Z. Anorg. Allg. Chem.* 1961, **313**, 90; J. Witte and H. G. Schnering, *Z. Anorg. Allg. Chem.* 1964, **327**, 260.
47. J. Passmore, G. Sutherland and P. S. White, *J. Chem. Soc., Chem. Commun.* 1980, 330.
48. I. D. Brown, D. B. Crump and R. J. Gillespie, *Inorg. Chem.* 1971, **10**, 2319; G. Cardinal, R. J. Gillespie, J. F. Sawyers and J. F. Vekris, *J. Chem. Soc., Dalton Trans.* 1982, 765.
49. T. W. Couch, D. A. Lokken and J. D. Corbett, *Inorg. Chem.* 1972; **11**, 357; J. Beck, *Z. Naturfor.* 1990, **45b**, 413, 1610.
50. G. E. Quelch, H. F. Schaefer III and C. J. Marsden, *J. Am. Chem. Soc.* 1990, **112**, 8719.
51. D. S. Warren and B. M. Gimarc, *J. Am. Chem. Soc.* 1992, **114**, 5378.
52. J. Donohue, A. Caron and E. Goldish, *J. Am. Chem. Soc.* 1961, **83**, 3748; J. Steidel, J. Pickardt and R. Steudel, *Z. Naturfor.* 1978, **B33**, 1554.
53. Y. Miyamoto, *Jap. J. Appl. Phys.* 1980, **19**, 1813.
54. B. Krebs, M. Hucke and C. J. Brendel, *Angew. Chem., Int. Edn Engl.* 1982, **21**, 445.
55. A. Almenningen, H. D. Martin and T. Urbanek, *J. Molec. Struct.* 1983, **128**, 239.